Progress in Aerospace Sciences 71 (2014) 150–166

Contents lists available at ScienceDirect

Progress in Aerospace Sciences

journal homepage: www.elsevier.com/locate/paerosci

Civil aircraft vortex wake. TsAGI's research activities

S.L. Chernyshev [a,b,*], A.M. Gaifullin [a,b], Yu.N. Sviridenko [a]

[a] Central AeroHydrodynamic Institute n.a. prof. N.E. Zhukovsky (TsAGI) 1, Zhukovsky str., Zhukovsky, 140180 Moscow Region, Russia
[b] Moscow Institute of Physics and Technology (MIPT) 9, Institutskii per., Dolgoprudny, 141700 Moscow Region, Russia

ARTICLE INFO

Article history:
Received 17 June 2014
Accepted 20 June 2014
Available online 18 August 2014

Keywords:
Vortex wake
Turbulence
Flight simulator

ABSTRACT

This paper provides a review of research conducted in TsAGI (Central AeroHydrodynamic Institute) concerning a vortex wake behind an airliner. The research into this area of theoretical and practical importance have been done both in Russia and in other countries, for which these studies became a vital necessity at the end of the 20th century. The paper describes the main methods and ratios on which software systems used to calculate the evolution of a vortex wake in a turbulent atmosphere are based. Verification of calculation results proved their acceptable consistency with the known experimental data. The mechanism of circulation loss in a vortex wake which is based on the analytical solution for the problem of two vortices diffusing in a viscous fluid is also described. The paper also describes the model of behavior of an aircraft which has deliberately or unintentionally entered a vortex wake behind another aircraft. Approximated results of calculations performed according to this model by means of artificial neural networks enabled the researchers to model the dynamics of an aircraft in a vortex wake on flight simulators on-line.

Contents

1. Introduction

The investigation of vortex flows has always been one of the paramount challenges for the researchers of TsAGI. This is largely accounted for by the fact that professor N.E. Zhukovsky, an outstanding scientist in the area of aerodynamics, made a significant contribution to the evolution of vortex flow theory through establishing linkage between the aerodynamic lift that acts on aircraft and its vortex patterns properties [1]. Experimental research on separated and vortical flows in wind tunnels, the numerical simulation of these phenomena, analytical studies in this area, and the generation of mathematical and engineering models constitute the scope of everyday scientific and technical activities of TsAGI. In 2013 the research Institute celebrated its 95th anniversary.

* Corresponding author at: Central AeroHydrodynamic Institute n.a. prof. N.E. Zhukovsky (TsAGI) 1, Zhukovsky str., Zhukovsky, 140180 Moscow Region, Russia. Tel.: +7 495 556 4172; fax: +7 495 777 6332.
E-mail address: slc@tsagi.ru (S.L. Chernyshev).

http://dx.doi.org/10.1016/j.paerosci.2014.06.004
0376-0421/

The second half of the XX century demonstrated a rapid development of trends that were related to the study of vortical flows; it was a period when major scientific schools, particularly the ones devoted to this branch, were established. It is well known that in high Reynolds number flows the separated boundary or the ablation layer decays in infinitely slender surfaces of tangential discontinuity in velocity. Nowadays numerical computational and analytical methods to investigate the flows of this nature within the perfect fluid model are well developed both in Russia and abroad. Two scientific schools played a particularly important role in the development of these methods in Russia and are still influential in TsAGI. One was headed by Nikolsky [2–4] and the other by Belotserkovsky [5–7]. The panel method and discrete vortices methods proved to be efficient when computing the forces and the moments that influence the streamlined body if the line of separation and the slide-off line are specified. But no matter how large the Reynolds numbers and how fine the space of flow discretization might be, there are particular areas with properties which are impossible to determine through these methods. Among them the core vicinity of spiral tangential velocity discontinuity, the flow separation points vicinity and the flow adjunction points vicinity, the vortical flows that evolve in large spatial and temporal scales and the vortical formations must be mentioned. Supplementing such methods of computing flows within inviscid fluid pattern with the research of flows parameters in particular areas will allow us to expand the range of solvable problems.

In this review we would like to dwell on the part of research of vortical flows related to the vortex wake behind high aspect ratio aircraft. This subject is not new to Russia. The solution to the far laminar wake problem can be found in a monograph by Landau and Lifshits [8]. They determined flow properties in relation to the lift and the drag acting upon the streamlined body. This problem received further development in the study of Ryzhov and Terentiev [9]. The results obtained belong to the stable wake phenomenon, whereas in practically important cases, for instance, in the case of the wake behind the high aspect ratio wing, the 3D vortex wake instability results in its structural change and decay.

The vortex wake problem became the subject of intensive investigations in TsAGI in the 1990 s. It should be mentioned that several research programs were simultaneously conducted in areas related to the determination of the characteristics of the wake itself, the simulation of atmospheric vorticity within which the vortex wake evolves, simulating the flow in a wake in wind tunnels, and studying the aircraft behavior in a wake behind another aircraft.

The aircraft behavior research covered the issues of flight dynamics, aeroelasticity and safety. Such activity was caused by the fact that the focus shifted from theoretical vortex wake research to practical flight research. The growth of passenger and cargo transportation made it necessary to study not only the traditional aspects of aircraft characteristics research, but both the issues of distance between landing aircraft which totally depends upon the wake characteristics; and also the aircraft behavior and training the staff to acquire the skills of controlling an aircraft that has entered an influence field of the vortex wake.

2. Zonal research method for vortex wake evolution

Nowadays the principal properties of the vortex wake behind a civil aircraft cannot be easily determined using any single numerical code. This problem is complex because its solution depends upon many non-uniformly scaled processes. The aircraft dimension is expressed in a few tens of meters, while a typical wake linear scale is of ten kilometers approximately, the atmospheric turbulence is characterized by one km scale; the diametrical wake size is about the wingspan, and the vortex core scale is about one meter. The flight altitude may vary significantly, e.g. from 10 km to several meters. It is problematic for a single equations system to describe all the processes that take place in a vortex wake. For that reason the major part of research conducted in TsAGI divides the total problem into subtasks.

From the point of view of flow zones differentiation one can distinguish two principal zones: (1) The area close to the aircraft and the near-field behind it; and (2) The long-distance zone where there is no aircraft and where the vortex wake evolves with specified characteristics.

The engineering methods [10,11], i.e. data approximation by simple algebraic or differential equations, were of a determining character at the initial stage of solving the problem. But step by step these solutions were replaced by numerical computation of more complex equations. Nowadays TsAGI possesses two major software packages that facilitate the computation of a vortex wake evolution, hereinafter referred to as Complex-1 and Complex-2 in papers [12–17], respectively. Attempts were made to calculate the flow within the vortex wake by the q–ω modified turbulence model [18,16].

2.1. Near wake

As far as the near-field is concerned, both Complexes are based upon the same approaches. The main objective is to determine the flow characteristics at the point of leaving the near field, that is, to determine the initial conditions for the far field.

The first three methods to determine the near-field flow properties require a rather detailed geometry of an aircraft. These methods are as follows:

1. The panel method for calculating equations for ideal fluid motion; and
2. The calculation that is based upon the total potential equations solutions subject to interaction with the boundary layer for transonic regimes or the calculation of 3D Reynolds-averaged (RANS) Navier–Stokes steady-state equations.

The panel method is based on PANSYM [19] and VORTPAN [20] codes developed by different programmers.

The aircraft surface is modeled in the PANSYM method by a number of quadrangular panels and the vortices and sources located on these panels. The fuselage surface is modeled by panels with a steady distribution of sources and sinks, and the panels with in-chord piecewise-linear distribution of vortex plane density and with piecewise-constant distribution of sources and sinks are located on the surface of the wing and fins. Engine jets are modeled by flow fields with panels with piecewise-constant distribution of vortex plane density at the border, which provides a drastic alteration of density and total pressure when crossing the boundary. The jet surface shape coincides with the flow streamlines and is determined in the course of the iterative solution of the flow problem. The computed angle of attack of an aircraft is determined by the weight, the speed and the altitude. The calculation model (e.g., IL-76 aircraft) in panel presentation is given in Fig. 1 where the computed shape of the vortex plane shed off the wing trailing edge and the tail plane, together with the geometry and the size of the engine jet flows, are shown.

The computed data vs. the experimental ones obtained under $M=0.60$ in WT for the IL-76 aircraft model are presented in Fig. 2.

In the VORTRAN method the aircraft surface is modeled by a set of panels. The wing is simulated by locating a net of vortical panels and the panels with continuously distributed sources on its mid-surface. The fuselage surface is modeled by panels with constant density sources; and the vortex plane is modeled by discrete

vortex lines. Two options for engine simulation are possible: it may be presented as a ducted nacelle or as a nacelle from which the jet is exhausted with specified excess velocity.

The BLWF code [21] is used to compute the vorticity distribution behind the aircraft in transonic flight. The program is based on a solution of the boundary-value problem for the velocity potential. The viscosity is considered by approximating the boundary layer with a fixed position of laminar-turbulent transition. The method allows one to model how local supersonic zones and shock waves emerge and facilitates the computation of flows with mild separation. The method is thoroughly validated.

The results obtained by panel methods turn out to be inapplicable to direct computing of the far wake because the vortex field is described by a set of vortical lines, each of infinite vorticity. Therefore, the vorticity of any vortex is "spread" upon the empirical formula onto some area. It is well known that turbulent jets which evolve in a homogeneous flow are described by parabolic equations. However, in reality the characteristics of the flow as a whole in the near field do not submit to parabolic equations. In papers [22,23,12] the fields of velocity and pressure are presented as a superposition of the field that is obtained by the panel method of computation and of the unknown field. For the unknown field the problem adds up to a parabolic equations system. The vortex structures obtained in such a way turn out to approximate the experimental data. Similarly, when using the BLWF code in order to describe the initial field the obtained distribution of circulation upon the lifting surfaces is being "spread" onto the trailing edges while taking into consideration the proper values of the boundary layer displacement thickness.

The k–ω SST turbulence model with wall function [24] is used as a model to close the turbulent equations for calculating the flow around the aircraft configuration by the solution of Reynolds-averaged Navier–Stokes equations. The zone problem discretization has been carried out by the second order accuracy pattern. The vorticity fields' patterns obtained when calculating the flow around the IL-76 aircraft configuration are given in Figs. 3 and 4.

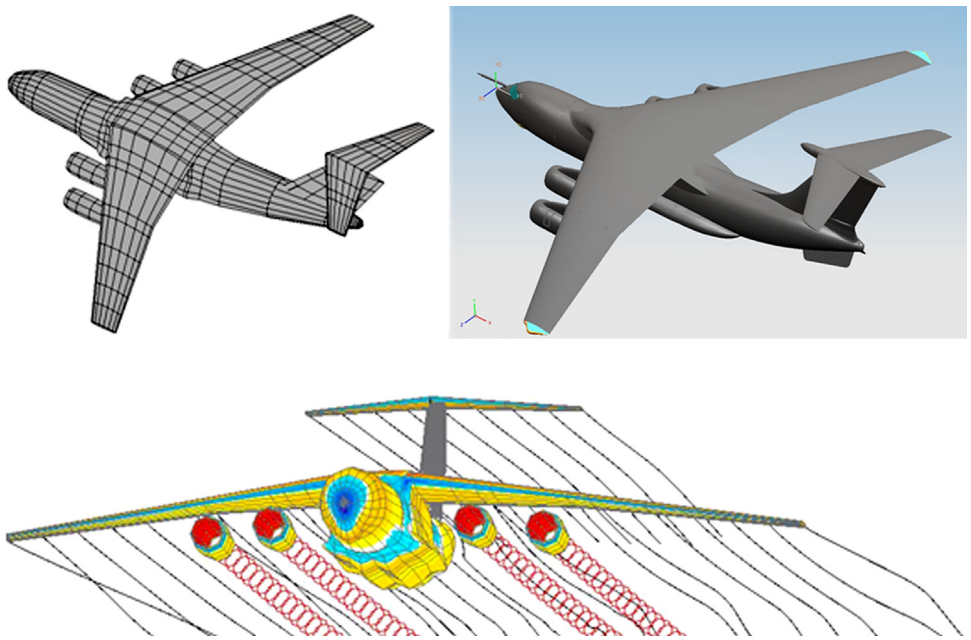

Fig. 1. IL-76 configuration in panel presentation.

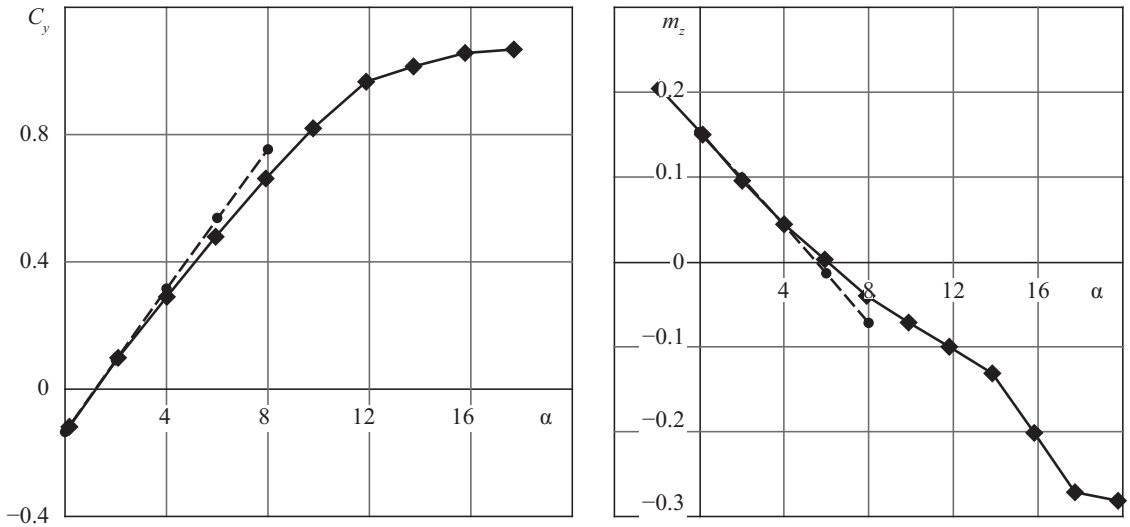

Fig. 2. The computed data vs. experimental ones obtained for IL-76 aircraft model; $M=0.60$; solid line denotes the experiment; the dotted line denotes the calculation.

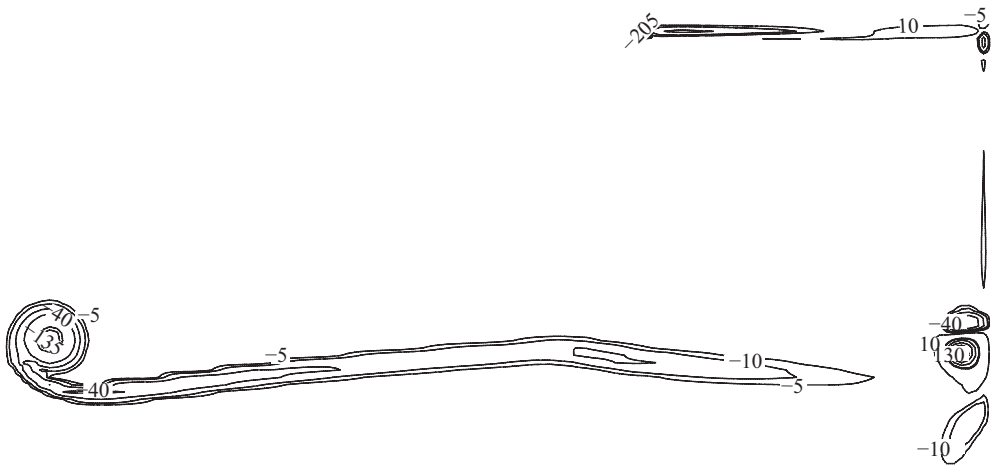

Fig. 3. Vorticity field three meters behind the aircraft (1/s).

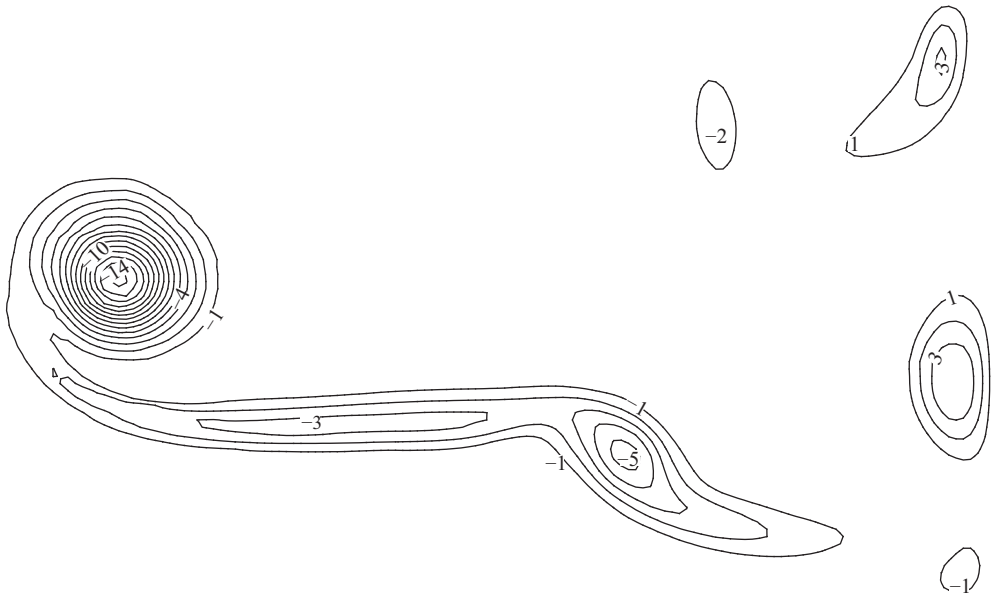

Fig. 4. Vorticity field one hundred and fifty meters behind the aircraft (1/s).

It should to be noted that vorticity diffusion/dissipation obtained during transition from the three meters cross-section to the cross-section of one hundred and fifty meters is higher than during the experiment. This is related to significant numerical viscosity on the lattices used for calculation. Therefore, the 3D RANS calculations were only used to obtain the initial field immediately behind the aircraft.

There are two other approaches to determine the flow characteristics at the near wake boundary: engineering models, e.g., the model [25] and the trial measurements. [14]. It is impossible to determine the near-wake flow characteristics by these approaches, they only allow to determine the characteristics in the section that is an initial section for the far wake.

2.2. Far wake

The far wake begins behind the aircraft at a distance that is approximately equal to the wing span. At such a distance it is possible to state that the longitudinal velocity and the temperature do not differ greatly from the approach flow velocity and the ambient temperature. Therefore, the unsteady analogy is applicable [26,4], according to which the 3D main approximation stable problem is substituted by the 2D unsteady problem by means of $t=x/u_\infty$ formal substitution. Both code complexes that allow calculation of the far-wake flow are based on the unsteady analogy application.

The calculation of the vortex jet wake by means of conventional Reynolds equations closure models results in high diffusion in the vortex cores [27,28]. Therefore, it was necessary to modify the turbulence models throughout Complex-1 and Complex-2.

Let us first describe Complex-1. In this code complex the fields of the following physical magnitudes are calculated: longitudinal vorticity, longitudinal velocity, temperature and integrated characteristics of turbulence.

The model in references [29–31] was specially generated to suit the calculation of vortex flows based on the invariant simulation approach that was developed at Princeton University under the leadership of Donaldson [32,33].

The equations for vortex jet wake turbulent flow calculation were derived in paper [30] under the assumption that the Λ-parameter is included in the equations and proportional to the size of extended turbulent vortices in the whole flow field. This parameter is called the turbulent flow macro-scale. Its importance for the vortex wake is described in paper [31]

$$\Lambda/b = 0.015. \quad (1)$$

Attempts to apply this model to vortex wake calculation resulted also in high diffusion of flows in the vortex cores. To eliminate this drawback it was decided [34] to abrogate the consistency of Λ-parameter and to consider it as dependent upon the longitudinal vorticity field characteristics. In such a case simultaneous equations for calculation of averaged turbulent flow functions [12–14] change.

The Λ-magnitude acts the part of efficient turbulent viscosity. The higher Λ-parameter is, the quicker the heterogeneities in fields of vorticity, longitudinal velocity and temperature decay. The re-laminarization of flow is observed even in the vortex cores, i.e., the sharp reduction of turbulent viscosity and hence of Λ-parameter.

It is evident that in the immediate vicinity of the aircraft vortex core the turbulent field of the vortex itself should prevail over the atmospheric turbulence and Λ should be proportional to the distance to the vortex core (radius). The Λ-parameter was assumed to depend upon the flow vorticity. The task is to match this magnitude value to the vorticity distribution. Thus, let Λ satisfy Eq. (1) when far from the vortex center and be proportional to the radius near to it. Let us construct the composite value of this magnitude within the total flow field. The simulated vorticity contour $\omega(r)=\alpha e^{-\beta r^2}$ in the turbulent vortex core has been used for this purpose. This contour was close to the experimentally observed one. In $\omega(r)=\alpha e^{-\beta r^2}$: r means the distance to the vortex center; α and β are dimensional constants that are responsible for the vortex intensity and dimension. The solution for Λ is found as

$$\frac{\Lambda}{\Lambda_0}=\left\{\frac{(\omega_{\max}^2-\omega^2)^2}{C^4\Lambda_0^4(\Delta\omega)^2\omega_{\max}^2+(\omega_{\max}^2-\omega^2)^2}\right\}^{1/4}, \tag{2}$$

where Λ_0 is calculated using (1), C — is a still to be determined unknown non-dimensional constant; $\omega_{\max}$ — is the maximum vorticity in the vortex core; Λ — is the Laplace operator.

Far away from vortex centers $|\omega|\ll\omega_{\max}$, so $\Lambda\approx\Lambda_0$. When $r\to 0$ $\Lambda\to r/(\sqrt{2}C)$. The numerical value of the unknown constant was found by comparing experimental data to computational ones

$$C=5. \tag{3}$$

The turbulence model (1)–(3) is effective in simulation of both full-scale experiments and wind tunnel ones using the same constant (3).

The given model may be generalized for the case of vortex development in ground surface vicinity. It is known that in wall vicinity

$$\Lambda=\alpha z. \tag{4}$$

The α factor is proportional to the Karman constant to [33] $\alpha=1.68\kappa$.

The numerical value of $\kappa\approx 0.4$ [35], therefore $\alpha\approx 0.67$.

In the case of vortex development in the bottom layer it is necessary to use a composite formula for the Λ magnitude satisfying the following three conditions. In the ground surface vicinity this formula is to turn into formula (4); in the vortex center vicinity it is to turn into formula (2) and far away from the vortex centers and the ground surface it is to turn into formula (1). In contrast to formula (2) in the ground surface vicinity the Λ magnitude must also depend on the distance to ground.

The following two-level composite formula has been chosen:

$$\frac{\Lambda}{\Lambda_0}=\left\{\frac{(\omega_{\max}^2-\omega^2)^2}{C^4\Lambda_0^4(\Delta\omega)^2\omega_{\max}^2+(\omega_{\max}^2-\omega^2)^2+(\Lambda_0/0.67z)^4(\omega_{\max}^2-\omega^2)^2}\right\}^{1/4},$$

for $z<z_0$

$$\frac{\Lambda}{\Lambda_0}=\left\{\frac{(\omega_{\max}^2-\omega^2)^2}{(C^4\Lambda_0^4(\Delta\omega)^2\omega_{\max}^2+(\omega_{\max}^2-\omega^2)^2)\exp(1-(z_0/z))+(\Lambda_0/0.67z)^4(\omega_{\max}^2-\omega^2)^2}\right\}^{1/4}.$$

For the calculations the z_0 value has been set equal to 20 m.

As a rule, at low altitude the aircraft is in the take-off and landing mode. In this case the lift devices are deflected and the multivortical system emerges behind the aircraft. Vorticity is generated by the vortex wake and the wind (the surface boundary layer).

The atmosphere may be in various conditions and due to this fact various undisturbed wind velocity profiles and the temperature profiles are possible as well. The classification of bottom layer wind is given in papers [36–38]. One of the simplest classifications distinguishes a stable state, a neutral state and an unstable one.

Now let us turn to Complex-2. Within this codes complex the longitudinal velocity field is considered homogeneous and equal to the free stream velocity. The fields of vorticity, temperature and integral characteristics of turbulence are computed. The calculation is performed by means of the turbulent viscosity algebraic model or the modified k–ε model [15–17]. When the algebraic model is used the ν_τ turbulent viscosity coefficient is derived from a cubic equation that in turn is derived from the balance of generation and dissipation of turbulent energy

$$c_1^2\nu_\tau S^2+c_2^3\varepsilon=\frac{\nu_\tau}{l^4}, \tag{5}$$

where $c_1=0.0002$, $c_2=0.16$, $S=\left|\frac{\partial w}{\partial r}-\frac{w}{r}\right|$, w — peripheral velocity, $\varepsilon=0.125q/L$, q — RMS atmospheric turbulence fluctuation velocity, L — atmospheric turbulence scale, l — vortex turbulence scale. In this case we have $l\ll L$. Turbulence scale l, as in Complex-1, is not constant and changes according to the following rule:

$$l^2=l_0^2\frac{S}{\sqrt{c_\omega\omega^2+S^2}}, \tag{6}$$

here we have $c_\omega=10$, $l_0=\sqrt{s_0/\pi}$, s_0 — area occupied by the vortex, i.e. the area where 99% of total circulation is concentrated, ω — vorticity.

The modified k–ε turbulence model case. This model is used as RNG (ReNormalization Group). To eliminate high vortex center diffusion the formula is modified for ν_τ turbulent viscosity coefficient

$$\nu_\tau=C_\mu\frac{k^2}{\varepsilon}\frac{1}{\sqrt{1+c(\omega k/\varepsilon)^2}}, \tag{7}$$

where $C_\mu=0.0845$, k — turbulence energy, ε — turbulence energy dissipation rate, and ω — vorticity.

Complex-2 can also be used to calculate wake evolution during flight in ground vicinity. Similarly to Complex-1, the state of the turbulent atmosphere is divided into stable, neutral and unstable states. The main characteristics of the wind profile, turbulent energy and turbulence energy dissipation rate are calculated by means of the Monin–Oboukhov model [39,40].

2.3. Codes Complexes verification

Both Codes Complexes for calculating a vortex wake behind the aircraft have been thoroughly verified to provide the correspondence of computed data to experimental measurements. Besides, numerical calculations have been verified by wind-tunnel and full-scale tests.

It should be noted that even under identical integral characteristics of the turbulent atmosphere its local properties along the vortex wake extension will be different. Hereupon there are two ways to calculate the vortex wake evolution in the turbulent atmosphere. The first one is related to modeling the characteristics of a wake that is located in a specifically pre-disturbed state of the turbulent atmosphere [25]. After performing a large number of such calculations under identical integral characteristics of

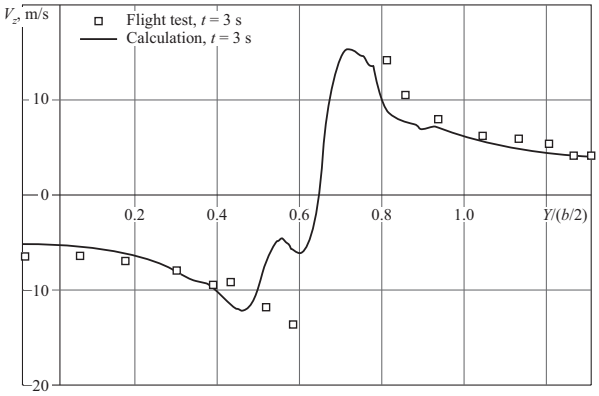

Fig. 5. Experimental data vs. the calculated ones in wake behind A-321 aircraft; 3 s after aircraft passage. $u_\infty=60$ m/s.

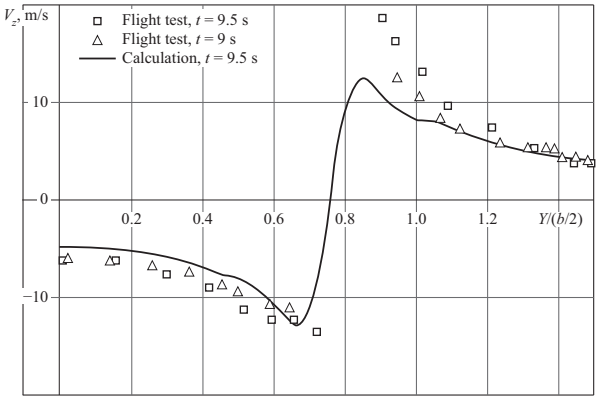

Fig. 6. The experimental data vs. the calculated ones in wake behind A-321 aircraft; 9 s after aircraft passage. $u_\infty=60$ m/s.

turbulence but under its different local ones it is possible to obtain averaged wake characteristics and their deviations from the average state. The second way is related to a direct calculation of the averaged wake characteristics. Both Complexes are generated on this basis. For both approaches the calculation may drastically differ from experimental data as the latter may also be considerably different from average values. This fact is confirmed by the results of paper [25], which describes two analyses of the wake characteristics behind a B757 aircraft. In the first analysis the turbulence energy dissipation rate differed from experimentally measured one by 4.6; and in the second one it differed by 31.8. At the same time the characteristics of circulation decay in the course of time turned out to be closer to experimental characteristics in the second analysis.

Unfortunately, it is impossible to model the jet-vortex wake as a whole even in large industrial wind tunnels. Moreover, the wake characteristics experimentally obtained differ greatly from those obtained through full-scale measurements. This is due to different turbulent field parameters of free flow in the wind tunnel and in the atmosphere. In the course of experiments aimed at studying the wake only the characteristics related to a single process under consideration are measured, while the ones related to other processes are ignored. That is, the far-wake flow characteristics are rated, but the near-wake vortices influence is not. Therefore, the computational data and the experimental ones will be compared on the basis of a number of papers.

2.3.1. *Let us consider the basic comparison data*

Codes Complex-1. Paper [41] presents the results of measuring the velocity profile in a wake behind an A321-aircraft flying at high altitude. The ground effect may be neglected in this case. Figs. 5 and 6 show the measured vertical velocity profiles and the calculated ones by Codes Complex-1. The vertical velocity profiles are taken along the line that passes through the vortices' centers. The results obtained by means of the VORTPAN panel method have been used as initial data. The free flow velocity was $u_\infty=60$ m/s.

In the numerical computation the spatial increment was $\Delta y=\Delta z=0.16$ m; the time increment was $\Delta t=0.002$ s. The y transversal distance is made dimensionless by the wing semi-span. In flight tests the parameters were evaluated at intervals $t=3$; 9 and 9.5 s after the aircraft passage.

In flight tests the vortex formation circulation is determined by lidars. The circulation is usually measured by the circumference of the specified radius, the center of which coincides with the vortex center. The results of such measurements are given in paper [43] for the B757 aircraft. Unfortunately, it does not indicate the radius for the circulation measured. Therefore, three curves that correspond to radii of 5, 6 and 7 m are given in Fig. 7. The time value is equal to $t=0$ and corresponds to the time period when the aircraft flies across the section under consideration. The results obtained by means of the VORTPAN panel method were also used in this calculation as initial data. The free stream velocity was $u_\infty=60$ m/s. In the computation the spatial increment was $\Delta y=\Delta z=0.1$ m; and the time increment was $\Delta t=0.01$ s.

To verify the code in the case when the vortex wake evolution in ground vicinity is considered, the results obtained by means of the codes complex and those calculated by means of Large Eddy Simulation (LES) and published in paper [25] are used. The initial circulation, the profiles of wind and temperature have been taken from paper [25]. The analysis was made for the B757 and DC10 aircraft. Experimental data obtained by means of lidar are also given. These data have been taken from paper [25] as well. The comparison is made based on the following parameters: velocity profiles, circulation drop (averaged within 3–10 m of radius) and the vortices altitude above the ground surface. The airspeed is 70 m/s. The spatial increment in the numerical computation was $\Delta y=\Delta z=0.1$ m, the time increment was $\Delta t=0.01$ s. The temporal value $t=0$ corresponds to aircraft flight over the section under consideration.

Let us consider the data for the B757 aircraft. The flight altitude was $H=175.0$ m. The initial vortex circulation was $\Gamma_0=345$ m^2/s; the initial distance between vortices was $b=29.8$ m. The RMS turbulent fluctuations velocity was 0.125 m/s. The profiles of lateral wind and potential temperature are given in Fig. 8. Fig. 9–11 show a calculated velocity profile and the measured one for the times $t=15$, 30 and 80 s after the aircraft flight. The average circulation values vs. time are given in Fig. 12. The average circulation is determined as a radius circulation integral divided by the difference between the upper and bottom integral limits. The vortex height variation vs. time is given in Fig. 13, the vorticity field at $t=140$ s is given in Fig. 14. The vortices descend sufficiently within this period of time. The velocity that they induce on the

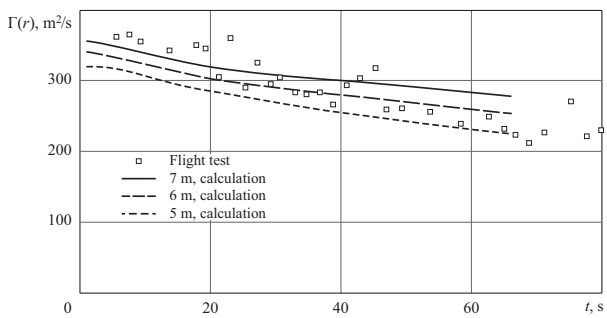

Fig. 7. Circulation decay in wake behind B757 aircraft.

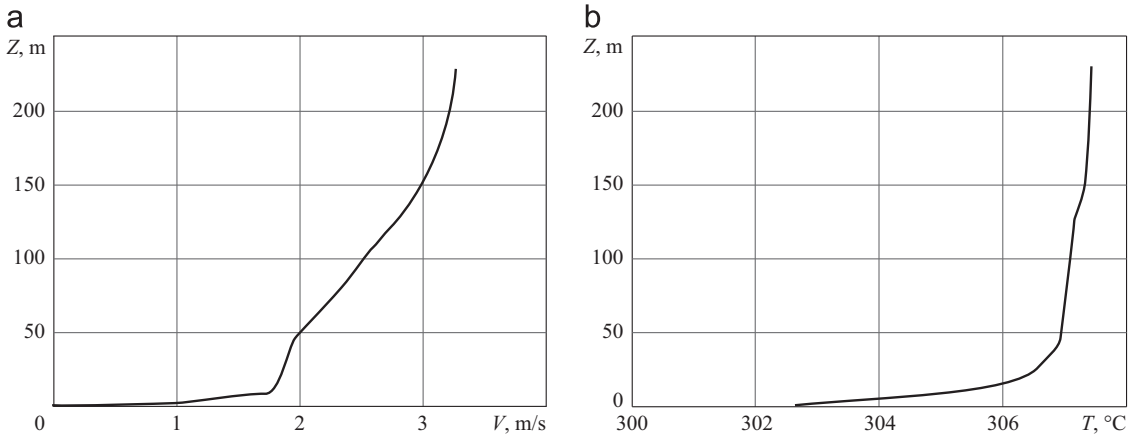

Fig. 8. Profiles: (a) lateral wind velocity and (b) potential temperature.

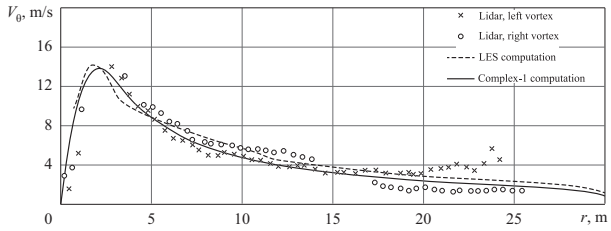

Fig. 9. Circular velocity profile in wake behind the aircraft B757 at $t=15$ s.

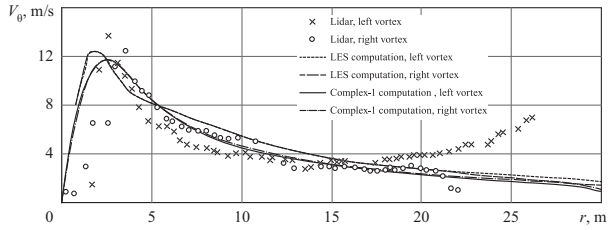

Fig. 10. The circular velocity profile in wake behind the aircraft B757 at $t=30$ s.

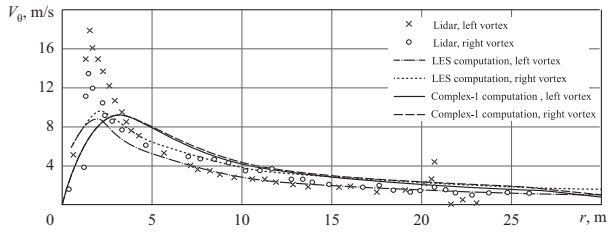

Fig. 11. Circular velocity profile in wake behind the aircraft B757 at $t=80$ s.

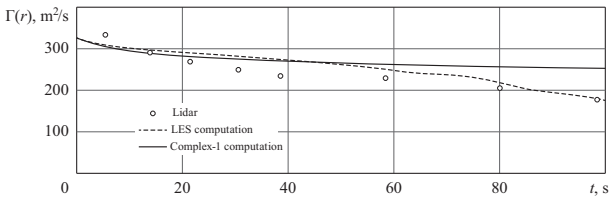

Fig. 12. 3–10 m radius circulation vs. time (B757).

ground surface becomes sufficiently high and the secondary vortices take off the ground surface.

The fields of vorticity and longitudinal velocity tested experimentally at TsAGI were also used to test the computation codes. The aircraft model was tested in the T-105 Wind Tunnel. The free stream velocity was 25 m/s. The velocity fields measured at cross section and

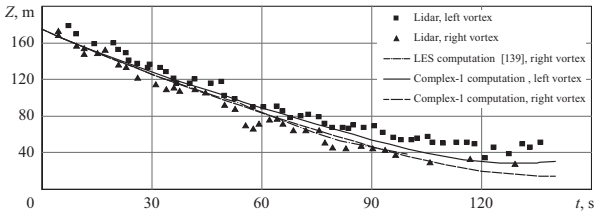

Fig. 13. Vortices height (B757).

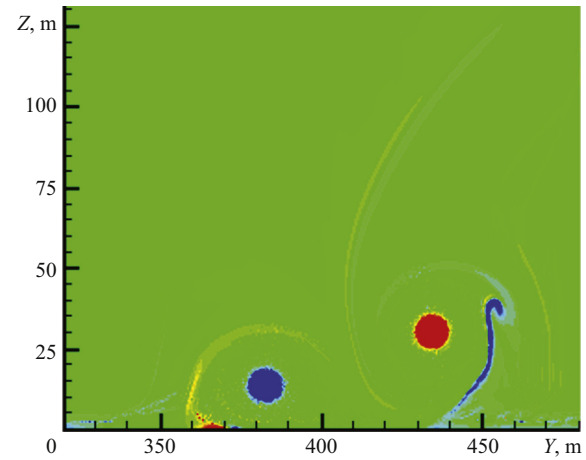

Fig. 14. Vorticity field at $t=140$ s (B757).

located at 0.6 spanwise from the wing were determined as the initial numerical calculation data. Turbulence intensity was set at $q=0.1$ m/s for the calculation. The calculation was carried out for a $\Delta y=\Delta z=0.006$ m spatial increment and $\Delta t=0.0002$ s time increment. The experimental data obtained in sections located 0.6 spanwise and 2 spanwise from the wing are given in Fig. 15(a) and (b) respectively. The computational vorticity field data obtained in the section located at the distance of 2 wing spans from the wing are given in Fig. 15(c). Similar data for longitudinal velocity are given in Fig. 16.

Now let us consider Code Complex-2. The location of vortices and the maximal vortex wake circular velocity were measured in the vicinity of the Frankfurt airport by means of lidars. In the course of it the aircraft flight moment and the data measuring time duration were recorded. The measured data and the data calculated by means of the k–ε turbulence model for the B747 aircraft flight are given in Fig. 17. The flight altitude was 65 m, the atmosphere was stable and the wind velocity was 4.6 m/s.

The approach was tested by means of the k–ε turbulence model when studying the wake behind the B757 aircraft [25].

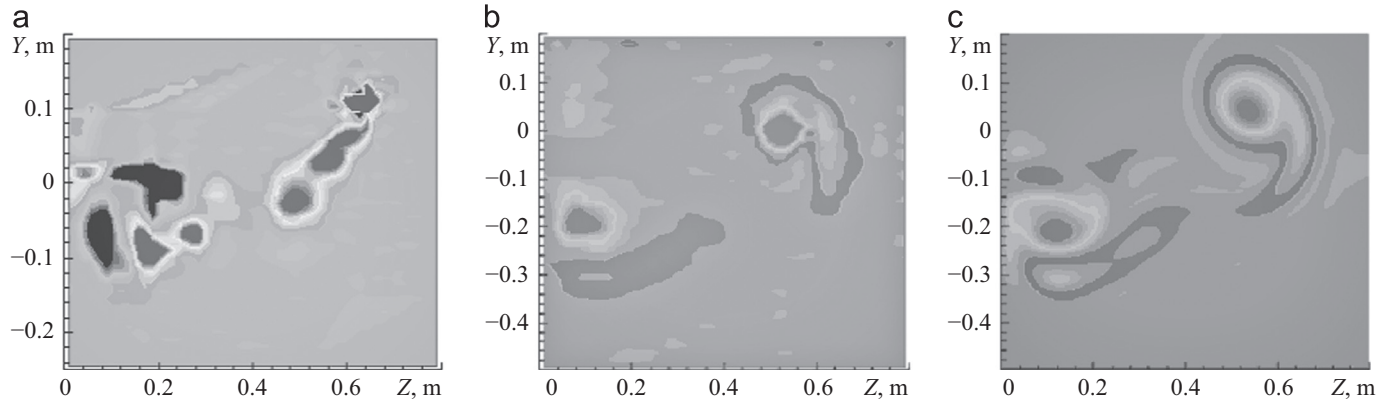

Fig. 15. Vorticity field: (a) field is measured in section as $x=0.6$ wingspan behind the wing and accepted as initial condition in numeric computation; (b) field is measured in section as $x=2$ wingspans behind the wing; (c) field is measured in section as $x=2$ wingspans behind the wing.

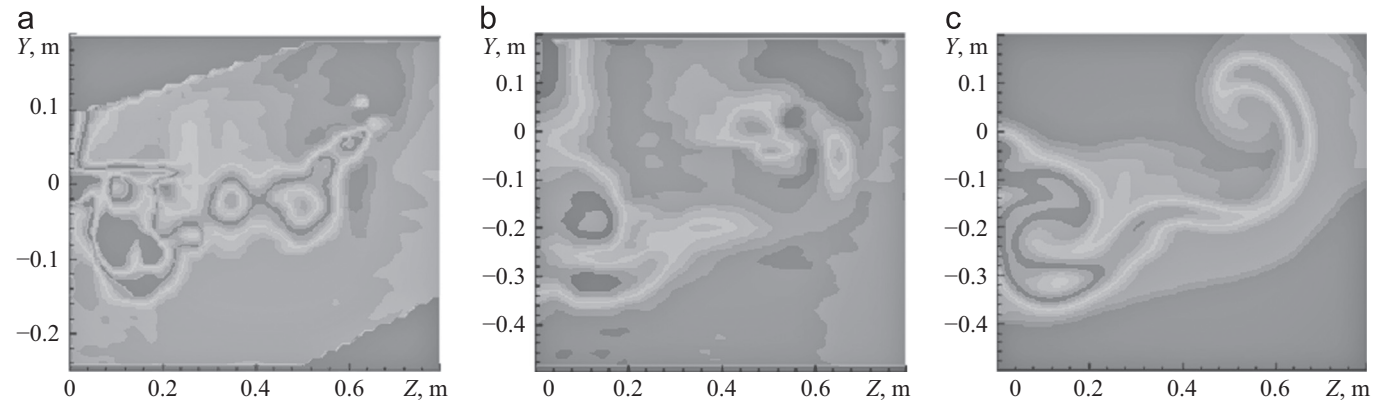

Fig. 16. Longitudinal velocity field: (a) field is measured in section as $x=0.6$ wingspan behind the wing and accepted as initial condition in numeric computation; (b) field is measured in section as $x=2$ wingspans behind the wing; (c) field is measured in section as $x=2$ wingspans behind the wing.

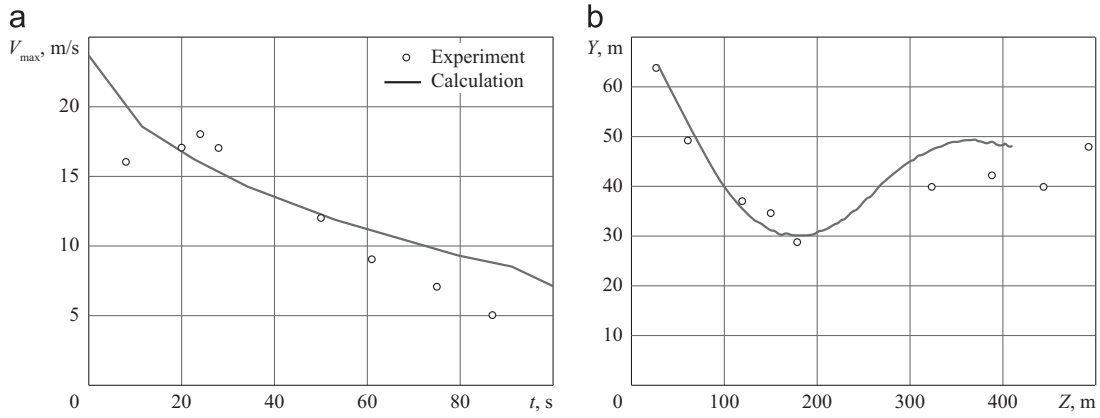

Fig. 17. Vortex evolution behind B747 aircraft: (a) maximal circular vortex velocity; (b) vortex path.

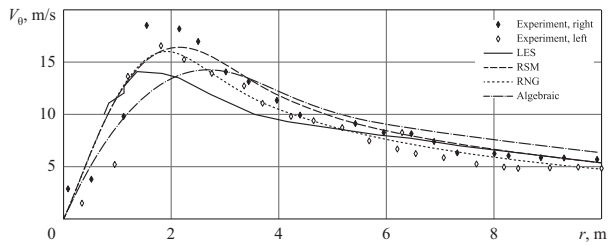

Fig. 18. Vortex wake behind B757 aircraft. Circular velocity in 15 s after aircraft flight.

The calculation was carried out for a neutral atmosphere and very low turbulence level. A comparison of computational data with the experimental data and with the data from paper [25] are given in Figs. 18 and 19.

3. Vortex wake instability and decay

A vortex wake exists for a long but finite period of time. Its finiteness is due to vortex wake instability. Depending on the turbulence atmosphere state the vortex wake behind the high

aspect ratio wing is intolerant to disturbances of certain wavelengths. The instability of various natures is generated by differences in vortex wake decay scenarios as well. Let us single out three decay scenarios.

The first and the most frequently observed scenario is the wake intolerance to long-wave (sinusoidal) disturbances. The $\lambda \sim 10b$ wave-length disturbances (b is the distance between vortices) develop quicker than other ones in an unstratified and low turbulent atmosphere. In accordance with experimental data given in paper [44] the atmospheric turbulence is $\varepsilon^* = (\varepsilon b)^{1/3}/V$ (where ε is a turbulence energy dissipation rate; V is a vortices descending velocity) and must be less than 0.05. The long-wave disturbances maxima and minima have a constant position in the frame of reference that is related to the ground observation station. At the same time the disturbance amplitude increases as the distance between the wake and aircraft becomes longer. In the frame of reference related to an aircraft the maxima and minima are shifting with the free stream velocity.

The second scenario takes place in an unstratified and highly turbulent atmosphere. It is a vortex "burst". It occurs at $\varepsilon^* > 0.1$. In this case the disturbance wave length is comparable to the vortex radius. A single vortex or two vortices at once may burst. The position of burst is constant in the frame of reference related to the aircraft. The vortex burst occurs due to inverse pressure gradient along the vortex line. The gradient increases as the sinusoidal disturbance amplitude grows. Both the first vortex wake decay scenario and the second one may take place in the $0.05 < \varepsilon^* < 0.1$ range.

The third scenario is observed in a steady stratified atmosphere [45]. The stratification behavior characteristic is the $N^2 = -(g/\rho_0)(d\rho/dz)$ Brunt–Väisälä frequency (where g is a gravitational acceleration; ρ_0 is a specific density, $d\rho/dz$ is a density change vs. altitude. The short-wave disturbances with the wave-length ranging from 1 to 2 spans between vortices start to prevail over the long-wave ones when the $\mathrm{Fr} = V/(Nb)$ Froude number diminishes. In the course of time the vortices' descending velocity decreases due to vortex circulation reduction; the Froude number decreases correspondingly and the short-wave disturbances growth rate increases. When the short-wave disturbance amplitude is sufficiently high a "coat" of 3-D eddying zones around the vortices is formed. The idea of such formations is given in colored figures in paper [46].

Other types of vortex wake instability are possible besides the above-mentioned ones [47–49]. It is still not clear what role they play in the general landscape of vortex evolution and if they can cause vortex decay.

A paper by Crow [50] contains theoretical research on long-wave wake instability. It explains the mechanism causing sinusoidal disturbance by means of the simple model of two infinite vortex tubes and determines the frequencies for which the disturbance growth is a maximum.

In a paper by Crow and Bate Jr. [51] the turbulence is recognized as a cause of sinusoidal disturbances and the wake lifespan is estimated depending on the turbulent pulsation intensity. This theory predicts rather accurately the lifespan of a vortex wake if its parameters in the far field behind the aircraft are known. At the same time it is difficult to forecast these characteristics during, for example, the landing phase.

The stability of a pair of vortices above the screen is investigated in papers [52,53]. The sinusoidal instability problem is considered in a simplified manner in papers [50–53]. It is considered that the spatial evolution may be replaced by the temporal one in the main approximation due to the vortex wake extension. In this case it is believed that certain magnitudes, e.g. the distance between the vortices and their height are supposed to be independent of time, i.e., the disturbances develop in a constant environment. The amplitude is supposed to grow exponentially. Actually, the distance between the vortices and their height is changing all the time, especially when moving over the underlying surface. This noticeably affects the sinusoidal disturbances growth up to the level that the specified frequency disturbances have progressive and damping periods in their evolution as they move away from the aircraft.

Papers [54,55] consider the spatial instability of a vortex wake in the vicinity of the ground surface both in an ideal fluid and a turbulent atmosphere.

3.1. Ideal fluid

The problem statement is as follows: the motion of two oppositely swirled vortex structures under the influence of self-induction in the presence of the underlying surface that simulates the ground surface is considered. It is assumed that we know the vortical tubes' path when there are no unstable disturbances that would affect vortical tubes. Such an "undisturbed" path may be obtained by numerical calculation. Let $f(t,x)$ and $g(t,x)$ be the right vortex deviations from the undisturbed motion (Fig. 20). The disturbed motion of the vortices may be represented as a superposition of symmetrical and skewed motions. The surface influence is simulated by reflected vortices.

Let the disturbances be presented as a wave running at u_1 velocity

$$g = A(x)\cos(\nu(x-u_1 t)+\delta_2), \quad f = B(x)\cos(\nu(x-u_1 t)+\delta_2),$$

where $A(x)$ and $B(x)$ are slowly rising functions. It is easy to obtain the $A(x)$ and $B(x)$ functions transform sequencing from the wake's geometric dimensions. At the X-length scale where the aircraft vortex wake is dissipating up to its decay these functions are changing at a rate equal to the order of initial vortices' span in the $x=0$ section. The $A(x)$ and $B(x)$ functions are presented as F and G functions that depend on a new variable $\eta = x/X$; the initial

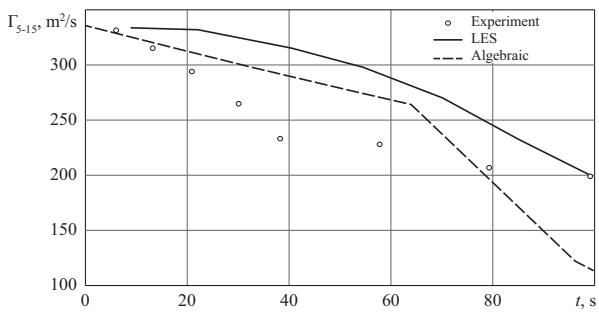

Fig. 19. Vortex wake behind B757 aircraft. The wake circulation loss.

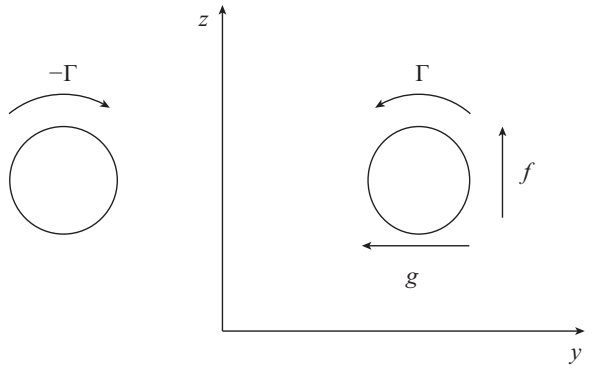

Fig. 20. Frame of reference and positive directions of disturbances.

distance between vortices is $b(0)$

$$A(x) = b(0)F(\eta), \quad B(x) = b(0)G(\eta)$$

It is demonstrated that the long-wave disturbances will be observed if and only if $u_1 \approx u_\infty$. The sinusoidal instability is related to the wave that "is runnig away" from the aircraft at u_∞ velocity. An observer on the ground surface will see a quasisteady-state evolution of sinusoidal instability. For him the wave in the fixed spatial point will remain in the same phase up to its decay, but the wave amplitude will change.

The $A(x)$ and $B(x)$ functions change in accordance with the general differential equation types which are obtained both for symmetric and skewed motion. The characteristics of the vortices are taken into consideration, i.e., the altitude of the vortices above

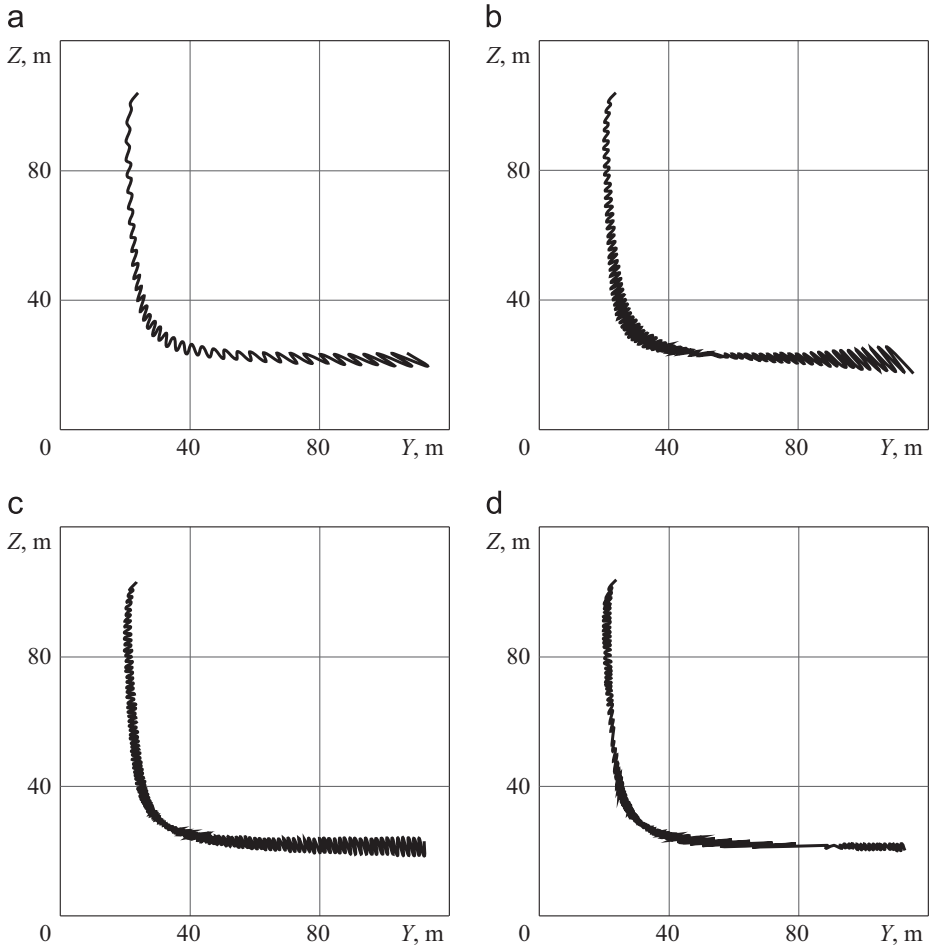

Fig. 21. Vortex wake evolution scenario (back view): (a) $\nu=0.01^{-1}$, (b) $\nu=0.02^{-1}$, (c) $\nu=0.03^{-1}$, and (d) $\nu=0.04^{-1}$.

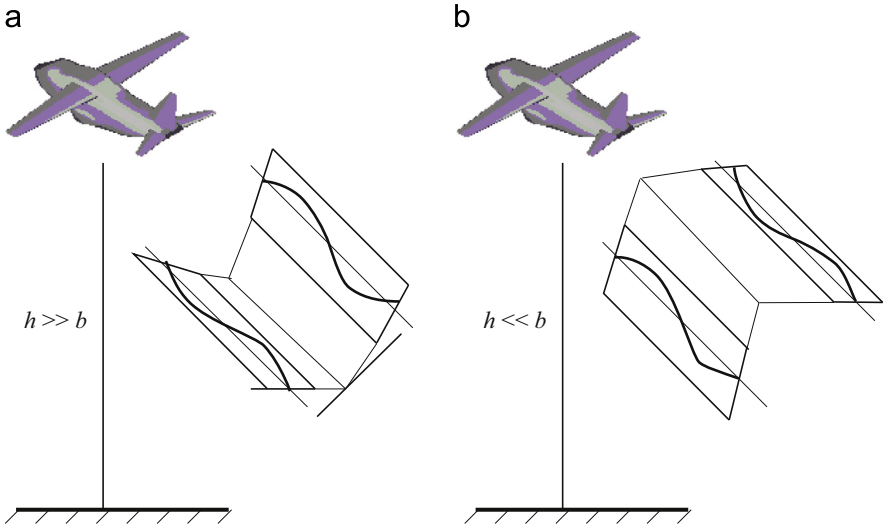

Fig. 22. The planes where the disturbances are propagating that correspond to maximum growing wave-numbers: (a) $h \gg b$ and (b) $h \ll b$.

the ground (h), the distance between the vortices (b) and the radius distribution of circulation and the possible variation of this magnitude during the wake's ageing.

These simultaneous differential equations were solved numerically to obtain the properties of the wake behind the B747 aircraft. It turned out that the amplitude of sinusoidal disturbances depends on many parameters. Moreover, when the parameters change, not only the amplitude, but also the scenario of vortex wake instability development may change. Vortex wake evolution scenarios (back view) under different frequencies of external disturbance factors are given in Fig. 21. The aircraft flight altitude is 100 m; the initial amplitude is of 0.5 m along Y-axis and 0.5 m along Z-axis.

When $\nu=0.01\ \mathrm{m}^{-1}$ the disturbance amplitude is continuously growing (Fig. 21(a)). When $\nu=0.02\ \mathrm{m}^{-1}$ (Fig. 21(b)) and $\nu=0.03\ \mathrm{m}^{-1}$ (Fig. 21(c)) the disturbances' amplitude is first growing then it drops and after that it continues to grow. When $\nu=0.04\ \mathrm{m}^{-1}$ (Fig. 21(d)) a number of amplitude growth and drop phases have already been observed. These Figures demonstrate the vibrations plane evolution as the ground surface is approaching. The planes where the disturbances with maximum growing wave-numbers are propagating are given as a sketch in Fig. 22 (a) and (b).

The disturbances' amplitude growth dependence vs. the distance to the aircraft is given in Fig. 23(a). The value $\tilde{A}=\sqrt{A^2+B^2}$. The initial sinusoidal oscillations plane is inclined by 45° in reference to the horizon. Furthermore, the oscillation amplitude is growing and the oscillation plane inclination angle may vary. The inclination angle variation is given in Fig. 23(b).

The wave-numbers for which the disturbance amplitude is growing are in the $0<\nu<0.03\ \mathrm{m}^{-1}$ range that corresponds to $4.9b<\lambda<\infty$ wave lengths. The maximum rise is observed when $\nu\approx(0.017\ldots0.018)\ \mathrm{m}^{-1}$ ($\lambda\approx 8.1b\ldots8.6b$), but this maximum is rather sloping. The disturbance amplitude vs. wave-number at $x=20$ km behind the aircraft is given in Fig. 24.

The amplitude growth rule that is calculated analytically and derived empirically is given in papers [50,56]. Based on the formulae obtained in these papers the amplitude of the sinusoidal disturbance oscillations behind a B747 aircraft will grow by e-times within 36.3 s [50] and 30.0 s [56]. In the paper under consideration this time corresponds to 37.2 s. But it is difficult to compare this magnitude with the empirically obtained one, as a large number of factors that influence wake evolution are not taken into account [57].

The $\lambda=2\pi/\nu$ wave-length corresponds to the ν wave-number disturbance. The $T=2\pi/\nu u_\infty=\lambda/u_\infty$ formula is the temporal period of aircraft vibrations as a solid body. The substitutional values ($\lambda\sim400$ m wave-length; $u_\infty\sim200$ m/s aircraft velocity) in the abovementioned formula will yield $T\sim2$ s. The aircraft oscillation with a period of $T\sim(1\ldots5)$ s will be called a short period oscillation. The motions of this type may be presented by the minor longitudinal motion when the angle of attack changes near the equilibrium state or by the minor lateral motion when the slip angle changes near the equilibrium state [58,59]. At the same time the study of the aircraft oscillation amplitude demonstrated that it is rather small and therefore it cannot provide the needed disturbances growth within the time period that is equal to the vortex wake lifespan for the known flight experiment.

Therefore, it is necessary to consider the evolution of the vortices in a turbulent rather than a quiet atmosphere [51]. This is done in papers [54,55]. The Karman turbulent energy spectrum is regarded as an atmospheric turbulence model

$$E(k)=\frac{55}{27\pi}q^2L\frac{(\alpha Lk)^4}{[1+(\alpha Lk)^2]^{17/6}},$$

where α is a constant that is equal to 1.339, L is a turbulence scale, and k is a wave-number.

The values of the turbulent disturbances are taken into account according to the papers [60,61]. The left and right vortices in turbulent atmosphere acquire additional velocity due to which both vortices either are on a head-on collision course or move away from each other in the horizontal plane, and the velocity due to which both vortices move in the vertical plane as an entity. The velocities of this type contribute to the disturbed symmetric motion of the vortices. Moreover, the vortices in turbulent atmosphere acquire additional velocity due to which both vortices move in a horizontal plane as an entity, and the velocity due to which both vortices move away one from the other in a vertical plane. The velocities of this type contribute to the disturbed asymmetric motion of the vortices.

Turbulent motion of a viscous medium constitutes a distribution of energy containing vortices. The growth rate of the disturbances in the wake behind an aircraft depends mainly on the vortices' strength, the l — linear size which is comparable with the size of $10b$ order. It is exactly the wave-length which the most

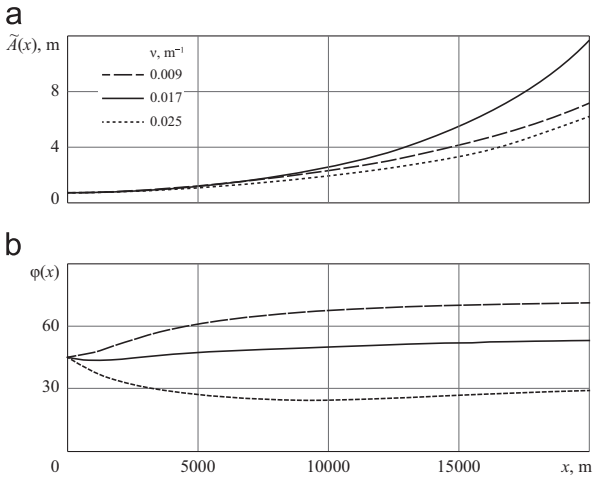

Fig. 23. The sinusoidal disturbances amplitude growth (a) and vibration plane inclination angle change (b) vs. the distance between the wake section and the aircraft.

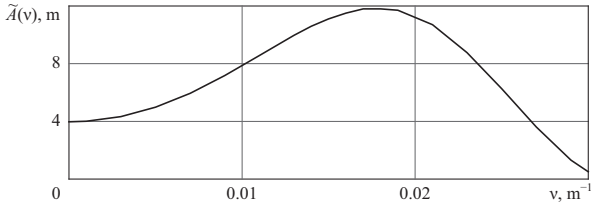

Fig. 24. The disturbance amplitude vs. wave-number at $x=20$ km behind the aircraft. When $x=0$ the disturbances amplitudes values are $A=B=0.5$ m.

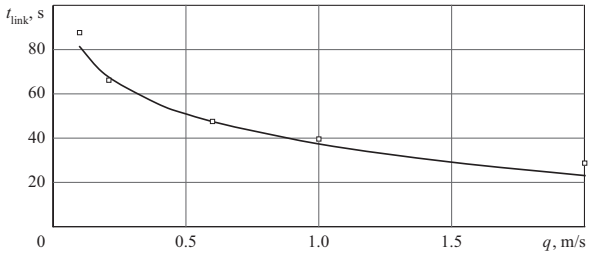

Fig. 25. The dependence of B757 wake lifespan on RMS turbulent fluctuations rate. The solid line denotes the empirical dependences [42,62], the markers - calculation [54,55].

rapidly growing disturbances have [50]. Under the specified RMS turbulent fluctuations rate the $t \sim l/q$ [33] typical vortices decay time is much higher than the wake lifespan. This fact allows us to roughly consider the vortex wake evolution in a "frozen" turbulent field.

As a result, the $A(x)$ and $B(x)$ amplitude disturbance growth is described by normal inhomogeneous differential equations, where the right parts depend on the turbulence integral characteristics. After finding the problem solution for each of the harmonic components it is necessary to obtain the superposition of these solutions. Doing this directly is impossible as the wave phases are random; they depend on a particular rather than integral state of the turbulent atmosphere. Therefore, the solutions are formed in terms of average.

A dependence of the t_{link} wake lifespan for the B757 aircraft in the landing configuration on the q — RMS turbulent fluctuations rate is given in Fig. 25. The dependence is determined by the given method (markers) and by empirical dependences [42,62] (solid line). The calculation by means of empirical dependences was performed for the following parameters: $\Gamma_0 = 335\ \text{m}^2/\text{s}$ is an initial circulation; $L = 220$ m is a turbulence scale. The proximity of the calculated curves to the empirical ones indicates the proximity of the former to the experimental data.

The growth rate of the short-wave disturbances is taken into account in the TsAGI Code Complexes according to [63].

4. Loss of vortex circulation in aircraft wake

In spite of a great number of published papers devoted to the aircraft vortex wake there are some problems in comprehending the physics of certain experimental results. The "loss" of circulation in vortices is one of these problems. The measurements made by means of lidars indicate that the vortices are weakening in the course of time: their circulation is alleviated, and the circulation alleviation rate depends upon the turbulence fluctuations intensity. The higher the RMS turbulent fluctuation rate is the faster the circulation is alleviated. An empirical formula of this dependence ($d\Gamma/dt = -0.82\Gamma q/b$) is given in paper [64].

In order to determine the physical origin of the circulation "loss" of the vortices a simplified problem was considered on two 2D oppositely rotating vortices in a viscid (laminar) fluid [65,66]. Initially both vortices are of a point nature. Such a vortex pair simulates the vortex wake behind the rectangular high aspect ratio wing [67]. The difference consists in the decay scenario. A three-dimensional vortex wake will decay due to a three-dimensional instability; and the circulation of the right or the left half of a two-dimensional vortical formation will be decaying in the course of time. Despite that, the physical origins of the circulation "loss" of the vortices should be expected to be the same for both cases.

At altitudes that are much higher than the distance between two vortices the vortices and the air descend jointly as an elliptical envelope in the course of time. The total circulation of the vortices is weakening in the course of time due to their interaction with vortices of the opposite sign. The diffusion is the main mechanism

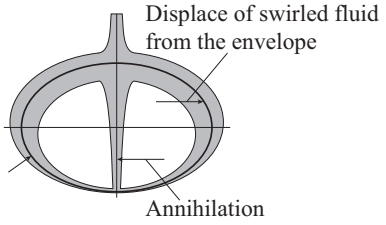

Fig. 26. Two mechanisms of vortices circulation loss.

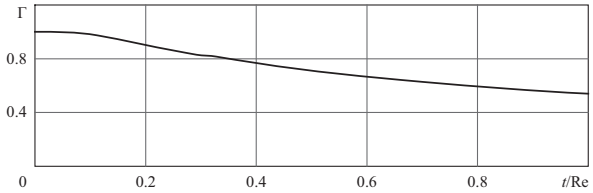

Fig. 27. Dependence of vortices' circulation on time.

of the circulation loss of the vortices in a laminar fluid. It is likely that for the vortex wake evolution in a turbulent atmosphere the circulation decay will be mainly determined by turbulent diffusion of the vortices as well. The vortex flow in a frame of reference descending together with the vortices is given in Fig. 26. Due to the turbulent diffusion the phenomenon of partial vorticity "annihilation" takes place: the opposite sign vorticity diffuses across the symmetry line of the elliptical envelope. This is the first way in which the vortices may lose circulation. Moreover, the vortices inside the envelope may be considered as a swirled fluid. The fluid is not swirled outside the envelope. Unstable turbulence distortions displace a portion of swirled fluid from the envelope. This portion is entrained by the external flow and moves upwards. This is the second way in which the vortices lose circulation.

The decrease of the circulation of vortices in a laminar fluid is given in Fig. 27.

5. Mathematical model of aircraft aerodynamics under vortex wake influence

The above-considered jet-vortex wake models were used to simulate the dynamics of the second aircraft entering a dangerous zone. During the simulation the problem of the second aircraft flying through a "frozen" wake field obtained by means of calculation was considered. Additional forces and moments conditioned by the jet-vortex wake influence on the second aircraft were determined in paper [13] according to the following algorithm:

1. The parameters of relative and angular positions of an aircraft in a wake were set.
2. Aerodynamic forces and moments in uniform flow were determined by means of a panel method.
3. The jet-vortex wake perturbed velocities were determined in panel test points by means of interpolation.
4. The flow analysis (the additional velocities were taken into account) was carried out; and the aerodynamic forces and moments were calculated.
5. The additional forces and moments were calculated by subtracting the values obtained at step-2 from the values obtained at step-4.

Thus the method of calculation was used to determine the increments of forces and moments that influenced the aircraft that flew into a jet-vortex wake area. While calculating the aircraft motion dynamics, the increments were calculated at each time step and added to the forces and moments taken from the bank of aerodynamic characteristics of the aircraft under consideration. Such an approach allows calculating the aircraft motion when flying into the jet-vortex wake of the other aircraft. But in order to simulate the unsafe flight situations by means of flight simulators or pilot training simulators it is necessary to create models that function in real time operation. The approach enabling real-time simulation is proposed in papers [13,68–72], where the creation of software modules which will be used to determine the additional

aerodynamic forces and moments acting on the aircraft entering the vortex wake influence area of another aircraft in the course of simulating the flight dynamics on a flight simulator is examined. To provide the high performance and the acceptable accuracy when determining the aerodynamic forces and moments the problem under consideration uses the simplified assumptions: forces and moments acting on aircraft are calculated in steady state; there are no lateral and vertical winds; the second aircraft influence on the characteristics and shape of the jet-vortex wake created by the first aircraft is not taken into account, and; the controls and the lift devices are in cruise configuration.

The algorithm chosen corresponded to the problem solution; it was formally staged as follows:

1. Characterizing the flow in the wake behind the first aircraft during cruise flight. The engine jets were taken into account in a calculation that was carried out using a certain basic regime by weight, flight altitude and velocity.
2. Recalculating the velocity field in vortex wake vicinity vs. weight, flight altitude and velocity. Calculation of additional forces and moments acting on the second aircraft vs. its spatial position in reference to the aircraft that generated the wake.
3. Carrying out the calculations of item 2 for a large number of random realizations of aircraft relative position, flight configuration and weight of the wake generator aircraft.
4. Forming the pattern population for training six neural networks that approximate the additional aerodynamic forces and moments acting on the second aircraft on the basis of item 3. Selecting topology and training the neural networks.
5. Accuracy evaluation of the approximations obtained.

Without using the neural networks, the calculation of additional forces and moments acting on an aircraft in a vortex wake (already calculated) requires about 10 s per point by means of a high-end PC. When using this data for simulating the refueling dynamics at the training simulator in real time for the characterization of the aerodynamic properties it is necessary to reduce the time required for determining the aerodynamic characteristics to 0.001 s, which is conditioned by the time integration step of the aircraft equations of motion. To solve this problem the approach based on approximating the obtained aerodynamic characteristics massive by means of artificial neural networks was used. Under such an approach the artificial neural networks that had been preliminarily trained using calculated data were employed as software modules for the aircraft aerodynamics in the mathematical software of the training simulator. This allowed reducing the time required for calculating the aircraft's wake characteristics significantly, with negligible determination accuracy.

Neural networks of multilayer perceptron with two buried layers type were used. The neural networks input vector contained both the three coordinate values of middle-haul aircraft in reference to the A380 and three angle values that described the aircraft angular position. The output vector was calculated by the increment of the aerodynamic forces and moments that were conditioned by the A380 wake effect. In total, six neural networks were trained to approximate three forces coefficients (C_d, C_L, C_y) and three moments coefficients (C_l, C_n, C_m).

About 100 000 calculations with random values of medium-haul aircraft positions in the A380 wake were performed in order to form a patterns population that was used to train and test the neural networks.

The general view of panel aircraft models and their positional relationship are given in Fig. 28. The total number of panels required to describe both aircraft models was about 1500. The calculations of the aerodynamic forces and moments that influenced the medium-haul aircraft were performed within the wide range of spatial and angular positions of this aircraft in reference to the A380 aircraft. The A380 airspeed value was assumed to coincide with the one of a medium-haul aircraft.

After training neural networks the accuracy of determining the increment to forces and moments generated when the aircraft entered into vortex wake zone was evaluated. The evaluation data obtained were compared to the computational characteristics obtained by the panel program. The following integrated evaluations of determining the accuracy of additional forces and moments were obtained; the RMS approximation errors deviations were:

$$\sigma(\Delta C_d) = 0.0010,\ \sigma(\Delta C_L) = 0.0160,\ \sigma(\Delta C_y) = 0.0019;$$

$$\sigma(\Delta C_l) = 0.0024,\ \sigma(\Delta C_n) = 0.0007,\ \sigma(\Delta C_m) = 0.0180.$$

In order to analyze the results the contour lines of forces and moments that influence the aircraft in the A380 vortex wake have been calculated. The patterns of lift variation contour curves when the aircraft is in *X*-sections that are 3000 m behind the other

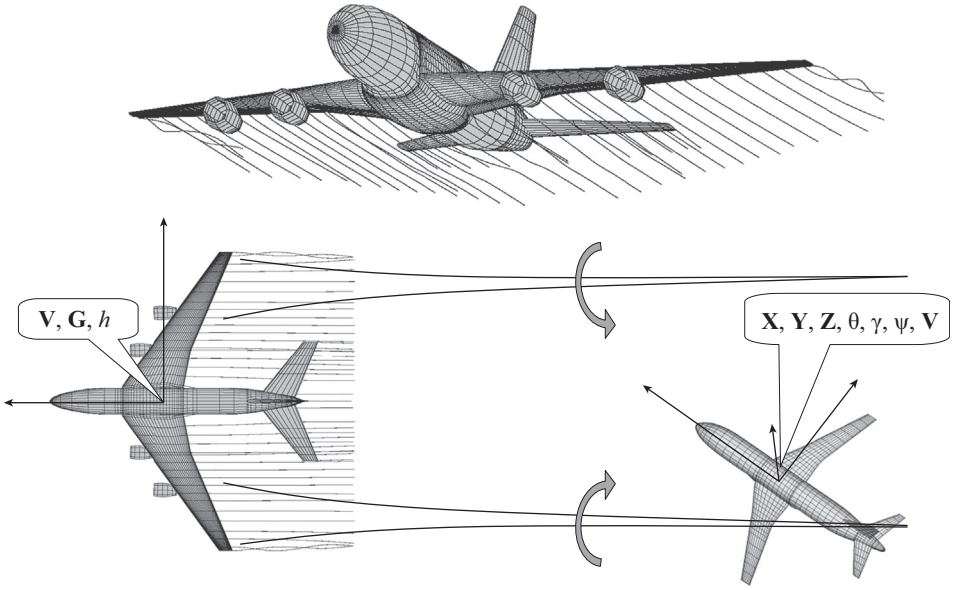

Fig. 28. Mathematical models of A380 aircraft and of medium-haul aircraft.

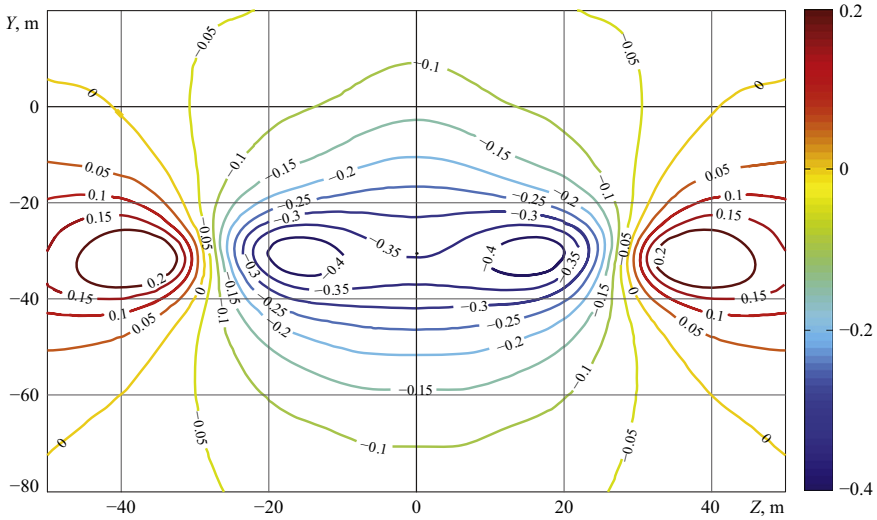

Fig. 29. Contour curves of the lift coefficient increment.

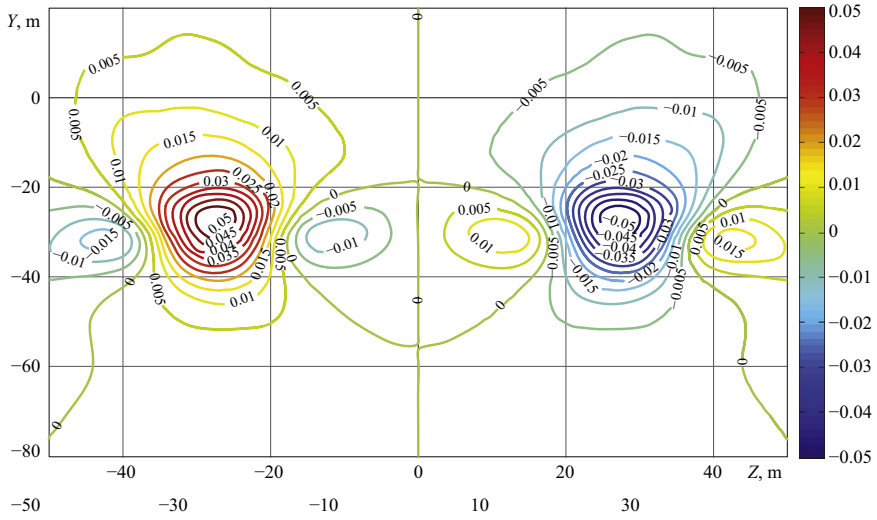

Fig. 30. Contour curves of the roll moment coefficient increment.

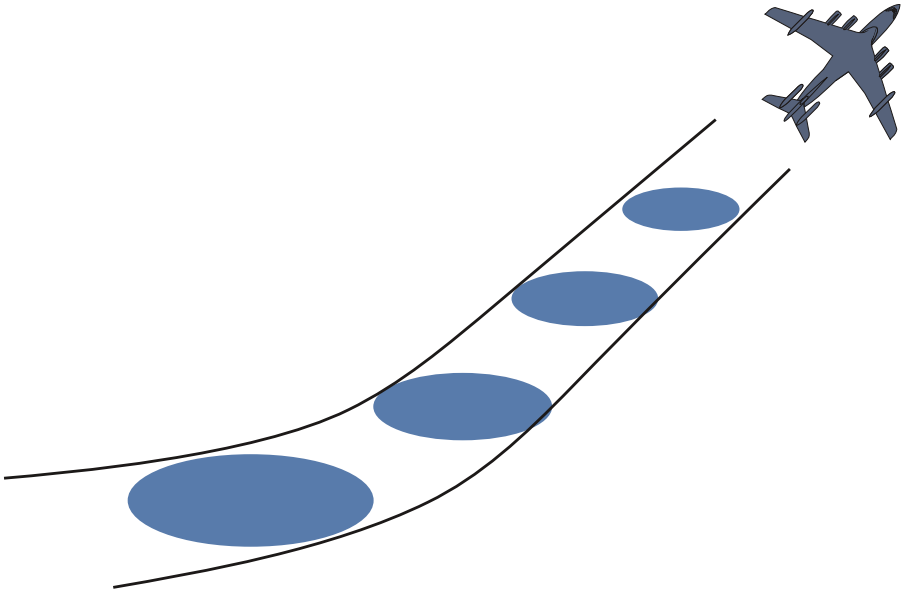

Fig. 31. The vortex wake is presented as a curved elliptical cone.

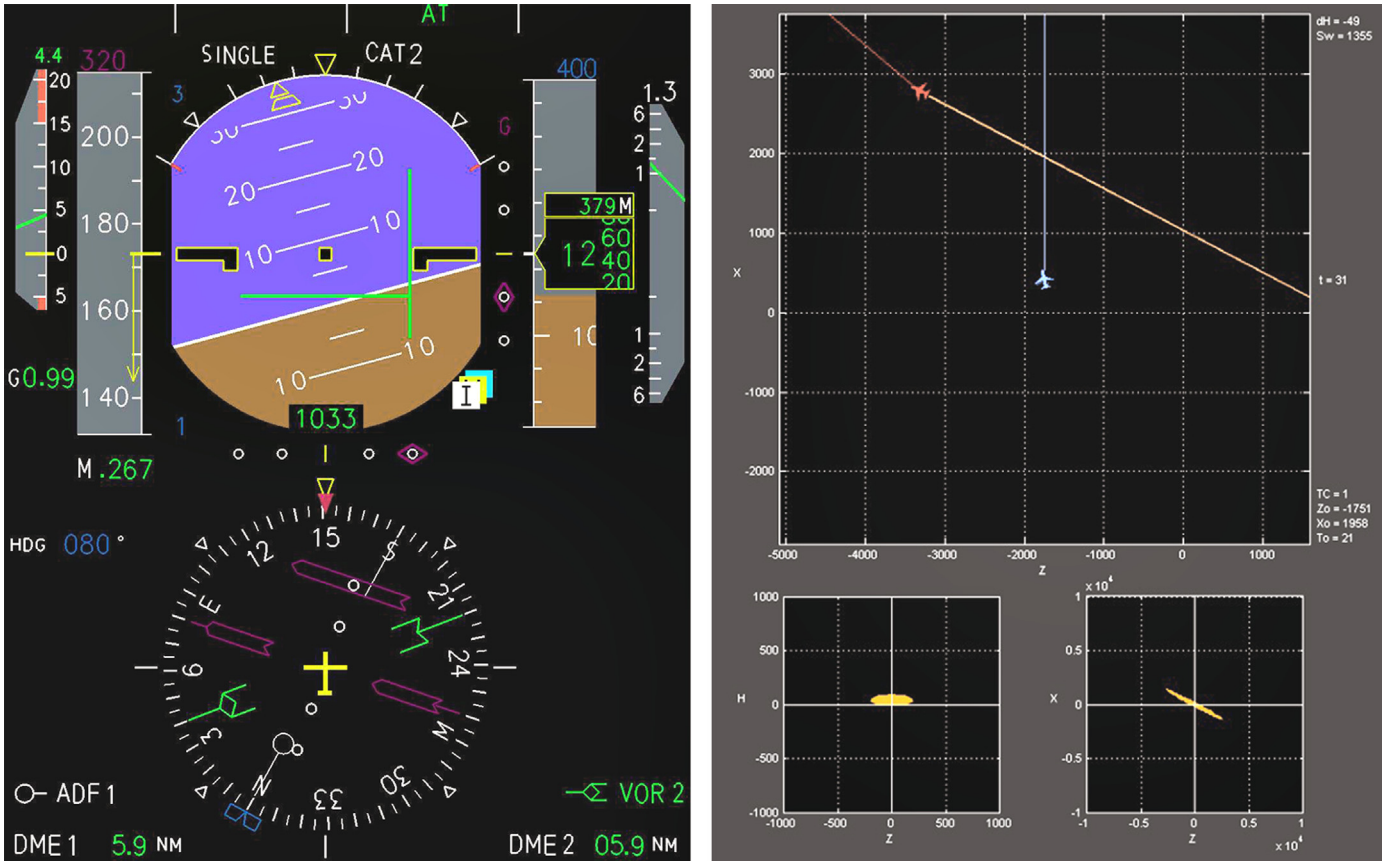

Fig. 32. Display system.

aircraft are given in Fig. 29. The patterns have been obtained by connectionist approximators. The aircraft airspeed was 236 m/s, the angle of attack was 2°, the angles of roll and heading were 0, respectively. The patterns of roll moment coefficient increment in relation to the aircraft's position in the wake are given in Fig. 30. The figures clearly show that the highest lift loss is observed when the aircraft is in the A380 aircraft symmetry plane; and the roll moment is under the most influence when the aircraft is close to the vortex core. To sum up, when the aircraft is within the vortex wake area it is influenced by the heeling and turning moments oriented towards the generator aircraft symmetry axis.

Key flight characteristics during cruise or in airfield vicinity are evaluated with significant error. In addition to the turbulence field characteristics, such parameters include the aircraft weight, its position, the wake instability parameters and wind velocity along the total wake evolution. The last parameter is the most important. Thus, if the wake lifespan is 200 s, the wind velocity in a given volume is known with 0.5 m/s accuracy, the error in determining the wake position may be 100 m. The concept of vortex wake calculation by probabilistic methods is presented in paper [73].

The type of probabilistic methods application in mathematical models developed for aircraft simulators is given in paper [68]. Let us describe the methods proposed. The vortex wake of the generator aircraft at cruise flight is dangerous only when the second aircraft is flying at a lower flight level. The upper aircraft must measure the horizontal wind components values by means of airborne devices and communicate the data obtained to the lower aircraft. In turn, the lower aircraft must measure the horizontal wind velocity components and assess the true vortex positions not long before encountering the collision point of the headings. Since the measurements are performed with errors (it may be assumed that they are of Gaussian distribution characterized by σ_{wm} RMS metering error) the positions of the vortices generated by the upper aircraft at the specified moment of time is determined by a certain ellipsoid where the wake may appear with a certain P probability. The envelope of these ellipsoids constitutes a surface similar to an elliptic cone (Fig. 31).

If the measurements indicate the presence of the lateral wind, the horizontal cone projection is skewed in reference to the upper aircraft's flight course. The thickness of this projection is proportional to the wing measurement computational error.

The model of twin-engine medium-haul aircraft was used to simulate the aircraft and vortex wake interaction by means of the PSPK-102 flight simulator and the supplementing PC-based mini-simulator. The visualization of the display system in the instrument panel is given in Fig. 32.

In order to distinguish between high and low vortex wake impact on the aircraft it is necessary to elaborate the quantitative criteria of this impact. Paper [68] put forward a “discomfort” parameter. The discomfort level is defined by the load factors and angular acceleration that influence the aircraft.

6. Conclusion

The description of the above-presented papers carried out at TsAGI highlighted mainly the topics of determining the properties of a vortex wake and its effect upon the aircraft behind it. At the same time, other problems associated with the vortex wake were considered at TsAGI: the atmosphere influence on the vortex wake evolution and on the additional vorticity generation [74]; the vortex wake properties control by means of circulation redistribution over the aircraft wing [75,76]; the particle motion within the

vortex wake [77–79]; the wind tunnel simulation of a vortex wake and its influence on the aircraft model [80–82]; the aircraft dynamic loading in a vortex wake [83–86], and; the aircraft dynamics conditioned by vortex wake influence [87,88].

Theoretical, computational and experimental research of vortex wakes behind aircraft is currently being conducted in TsAGI as well as other Russian institutions. This research is of increasing importance in light of the need to shorten the distances between aircraft.

References

[1] Zhukovsky NE. On bound vortices. Collected works, vol. 4. M.-L.: Gostechizdat P.H.; 1949. p. 69–71 [in Russian].
[2] Nikolsky AA. On the second motion shape of ideal fluid around streamlined body (stalling vortex flows research). F-EAS USSR, vol. 116, no. 2; 1957. p. 193–6 [in Russian].
[3] Nikolsky AA. On force influence of the second form of the hydrodynamic flow on 2D bodies (2D stalling flows dynamics). F-EAS USSR, vol. 116, no. 3; 1957. p. 365–8 [in Russian].
[4] Nikolsky AA. Similarity lows for 3D stable stalling flow around body by fluid or gas. Uchenye Zap. TsAGI 1970;I(1):1–7 [in Russian].
[5] Belotserkovsky SM. Slender airfoil in subsonic gas flow. Moscow: M.: Nauka; 1965 (244 p [in Russian]).
[6] Belotserkovsky SM, Nisht MI. Separated and attached flow around slender wings by ideal fluid. Moscow: M.: Nauka; 1978 (352 p [in Russian]).
[7] Belotserkovsky SM, Lifanov IK. numerical methods in singular integral equations and their application in aerodynamics, elasticity theory and electrodynamics. Moscow: M.: Nauka; 1985 (256 p [in Russian]).
[8] Landau LD, Lifshits EM. Theoretical physics. Hydrodynamics, vol. 6. Moscow: M.: Nauka; 1986; 736 [in Russian].
[9] Ryzhov OS, Terentiev ED. On lifting body wake in viscid fluid. PMTF, vol. 5; 1980. p. 83–91 [in Russian].
[10] Voyevodin AV, Gaifullin AM, Zakharov SB, Soudakov GG. Zonal calculation method for aircraft wake. Trudy TsAGI 1996;2622:54–65 [in Russian].
[11] Gaifullin AM, Soudakov GG, Voyevodin AV, Zakharov SB. Computation of flow in the wake behind a high-aspect-ratio wing. Trudy TsAGI 1997;2627:33–42.
[12] Voyevodin AV, Vyshinsky VV, Gaifullin AM, Sviridenko YuN. Evolution of civil aircraft jet-vortex wake. Aeromech Gas Dyn 2003;4:23–31 [in Russian].
[13] Gaifullin AM, Sviridenko YuN, Safronov PV. Mathematical model of aircraft model aerodynamics when being influenced by vortex wake. Trudy TsAGI 2008;2678:100–10 [in Russian].
[14] Gaifullin AM. Research of vortex structures that are formed when flowing around body by fluid or gas. Moscow: Publishing Department of TsAGI; 2006 (139 p [in Russian]).
[15] Vyshinsky VV, Soudakov GG. Mathematical model of aircraft vortex wake evolution in turbulent atmosphere. Aeromech Gas Dyn 2003;3:46–55 [in Russian].
[16] Vyshinsky VV, Soudakov GG. Aircraft vortex wake in turbulent atmosphere. Trudy TsAGI 2005;2667:1–156 [in Russian].
[17] Bobylev AV, Vyshinsky VV, Soudakov GG, Yaroshevsky VA. Aircraft vortex wake and flight safety problems. J Aircr 2010;47(2):663–74.
[18] Pakin AN. Application of a modified q-ω turbulence model to simulation of two-dimensional vortex gas motion. Trudy TsAGI 1997;2627:79–92.
[19] Sviridenko YuN, Ineshin YuL. Application of panel method with symmetrization of singularities for calculating flow around aircraft with regard to engine jets influence. Trudy TsAGI 1996;2622:41–53 [in Russian].
[20] Voyevodin AV, Soudakov GG. Method of calculating the aerodynamic characteristics of stalling flow around aircraft by subsonic gas flow. Uchenye Zap TsAGI 1992;XXIII(3):3–11 [in Russian].
[21] Kovalev VE, Karas OV. Calcul de l'écoulement transsonique autour d'une configuration aileplus-fuselage compte tenu des effects visqueux et d'une région décollée mince. La Rech Aérosp 1994;1:23–38.
[22] Zvonova Yu S, Gaifullin AM. Engine turbulent jet and aircraft vortex wake interference. Aviation Technologies of the XXI century: new challenges of aeronautical science. VI. Zhukovsky; 2001. p. 361–8 [in Russian].
[23] Gaifullin AM, Zvonova YuS, Sviridenko YuN. Calculation of engine turbulent jet and airframe. Trudy TsAGI 2002;2655:160–6 [in Russian].
[24] Bychkov IM, Kornyakov AA. Research of air refueller vortex wake. Nauchny vestnik of CA MSTU, vol. 138; 2009. p. 90–3 [in Russian].
[25] Shen S, Ding F, Han J, Lin Y-L, Arya SP, Proctor FH. Numerical modeling studies of wake vortices: real case simulation. AIAA paper 99-0755; 1999.
[26] Adams MC, Sears WR. Slender-body theory – review and extension. J Aeronaut Sci 1953;20(2):85–98.
[27] Kandil OA, Wong TC, Adam I, Liu CH. Prediction of near- and far-field vortex-wakes turbulent flows. In: Proceedings of AIAA atmospheric flight mechanic conference, AIAA 95-3470-CP. Baltimore; August 7–9, 1995. p. 415–25.
[28] Pakin AN. On choosing differential turbulence models for calculation of 2D gas vortex flows. Trudy TsAGI 1996;2622:90–9 [in Russian].
[29] Bilanin AJ, Teske ME, Williamson GG. Vortex interactions and decay in aircraft wakes. AIAA J 1977;15(2):250–60.
[30] Quackenbush TR, Teske ME, Bilanin AJ. Dynamics of exhaust plume entrainment in aircraft vortex wakes. AIAA paper 96-0747; 1996. 16 p.
[31] Hecht AM, Hirsh J, Bilanin AJ. Turbulent line vortices in stratified fluids. AIAA paper 80-0009; 1980. 21 p.
[32] Donaldson C, du P. Calculation of turbulent shear flows for atmospheric and vortex motions. AIAA J 1972;10(1):4–12.
[33] Frost W, Moulden T, editors. Turbulence. Principles and applications. M.: Mir P.H.; 1980, 535 p.
[34] Vyshinsky VV, Gaifullin AM, Zvonova YuS, Sviridenko YuN. Evolution and decay of aircraft jet-vortex wake. VI Aviation Technologies of the XXI century: new challenges of aeronautical science. Zhukovsky 2001:111–22 [in Russian].
[35] Schlichting G. Theory of boundary layer. Moscow: M.: Nauka; 1969 (744 p [in Russian]).
[36] Zilitinkevich SS. Dynamics of atmosphere boundary layer. L., Guidrometeoizdat P.H.; 1970 (292 p [in Russian]).
[37] Bütner EK. Dynamics of near-surface air layer. L.: Guidrometeoizdat P.H.; 1978 (160 p [in Russian]).
[38] Nyistadt FTM, Van Dopa KhL, editors. The atmosphere turbulence and modelling particles propagation. Guidrometeoizdat P.H.; 1985. 352 p [in Russian].
[39] Monin AS, Yaglom AM. Statistical hydromechanics. Part 1. Moscow: M: Nauka; 1965 (640 p [in Russian]).
[40] Byzova NL, Ivanov VN, Garger EK. Turbulence in atmosphere boundary layer. L.: Guidrometeoizdat P.H.; 1989 (263 p [in Russian]).
[41] Harris M, Vaughan JM, Huenecke K, Huenecke C. Aircraft wake vortices: a comparison of wake-tunnel data with field trial measurements by laser radar. Aerosp Sci Technol 2000;4:363–70.
[42] Sarpkaya T. New model for vortex decay in the atmosphere. J Aircr 2000;37 (1):53–61.
[43] Kopp F. Dopler lidar investigation of wake vortex transport between closely spaced parallel runways. AIAA J 1994;32(4).
[44] Sarpkaya T, Daly JJ. Effect of ambient turbulence on trailing vortices. AIAA paper 87-0042; 1987. 8 p.
[45] Delisi DP, Robins RE. Short-scale instabilities in trailing wake vortices in a stratified fluid. AIAA J 2000;38:1916–23.
[46] Holzapfel F, Gerz T, Baumann R. The turbulent decay of trailing vortex pairs in stable stratified environments. Aerosp Sci Technol 2001(5):95–108.
[47] Gaifullin AM, Soudakov GG. Aircraft vortex wake dynamics. AIAA paper 965547; 1996. 7 p.
[48] Betyaev SK. Mathematical simulation of vortices wakes dynamics. Trudy TsAGI 1996;2622:22–40 [in Russian].
[49] Betyaev SK. Mathematical models of nonaxisymmetric columnar vortex. Fundam Princ Chem Technol 2002;36(2):124–9 [in Russian].
[50] Crow SC. Stability theory for a pair of trailing vortices. AIAA J 1970;8 (12):2172–9.
[51] Crow SC, Bate Jr ER. Lifespan of trailing vortices in a turbulent atmosphere. J Aircr 1976;13(7):476–82.
[52] Kornev NV. Instability and non-linear dynamics of trailing vortices in an inviscid fluid over a solid surface. Fluid Dyn 1997;32(2):239–44.
[53] Kornev NV, Reichert G. Three-dimensional instability of a pair of trailing vortices near the ground. AIAA J 1997;35(10):1667–9.
[54] Gaifullin AM. Equations of perturbation growth in aircraft wakes. Fluid Dyn 2001;36(3):448–57.
[55] Gaifullin AM. Equations for the sinuous instability growth downstream an aircraft. Trudy TsAGI 1999;2641:148–61.
[56] Stuever RA, Greene GC. An analysis of relative wake-vortex hazards for typical transport aircraft. AIAA paper 94-0810; 1994. 15 p.
[57] Gaifullin AM, Voyevodin AV, Zakharov SB. Zonal method of aircraft wake calculation. Trudy TsAGI 1999;2641:111–20.
[58] Braga VG, Lyssenko NM, Mikirtumov EB, et al. Practical aerodynamics of turbo-jet aircraft. M.: Voenizdat P.H.; 1969 (408 p [in Russian]).
[59] Nikolaev LA. Aerodynamics and flight dynamics of transport aircraft. M.: Transport P.H.; 1990 (392 p [in Russian]).
[60] Kuzmin VP. Estimation of wake-vortex separation distances for approaching aircraft. Trudy TsAGI 1997;2627:209–24.
[61] Bobylev AV, Kuzmin VP, Yaroshevsky VA. Mathematical simulation of the wake vortices effect on aircraft motion during automatic landing. Trudy TsAGI 1997;2627:198–208.
[62] Sarpkaya T. Decay of wake vortices of large aircraft. AIAA J 1998;36(9):1671–9.
[63] Gerz T, Holzapfel F, Darracq D. Commercial aircraft wake vortices. Prog Aerosp Sci 2002;3:181–208.
[64] Greene GC. An approximate model of vortex decay in the atmosphere. J Aircr 1986;23(7):566–73.
[65] Gaifullin AM, Zoubtsov AV. Diffusion of two vortices. Fluid Dyn 2004;39 (1):112–27.
[66] Gaifullin AM, Zoubtsov AV. On diffusion of two vortices. Trudy TsAGI 1997;2627:102–22.
[67] Van Dyke M. Perturbation technique in fluid mechanics. Moscow: M.: Mir; 1967 (310 p [in Russian]).
[68] Yaroshevsky VA, Bobylev AM, Gaifullin AM, Sviridenko Yu N. Vortex wake influence on civil aircraft flight dynamics. Polyet. 90th anniversary of TsAGI; 2008. p. 93–9 [in Russian].
[69] Bobylev AV, Gaifullin AM, Sviridenko Yu. N, Yaroshevsky VA. Interaction of the aircraft with a vortex wake. 7th seminar TsAGI-ONERA; 2008. p. 14–5.
[70] Gaifullin AM, Sviridenko YuN. Mathematical model of aircraft dynamics in vortex wake. Uchenye Zap. TsAGI 2010;XLI(4):3–16 [in Russian].

[71] Gaifullin AM. Evolution and decay of civil aircraft jet-vortex wake. In: Proceedings of the mathematical center n.a. N.I. Lobachevsky, vol. 42; 2010, p. 75–91 [in Russian].
[72] Gaifullin AM, Sviridenko Yu N. Civil aircraft vortex wake. Vestnik of Nizhegorodsky University n.a. N.I. Lobachevsky, part 3, vol. 4; 2011, p. 697–9 [in Russian].
[73] Holzäpfel F, Robins RE. Probabilistic two-phase aircraft wake-vortex model: application and assessment. J Aircr 2004;41(5).
[74] Pavlenko AA. Influence of quiet atmosphere stratification on aircraft vortex wake evolution. Trudy TsAGI 1996;2622:81–9 [in Russian].
[75] Soudakov GG, Voeyvodin AV, Zubtsov AV. Alleviation of the vortex wake behind an aircraft. Trudy TsAGI 1999;2641:183–90.
[76] Pavlovets GA, Voeyvodin AV, Zubtsov AV. On the effect of spanwise circulation distribution on the vortex wake intensity. Trudy TsAGI 1999;2641:191–4.
[77] Znamenskay UP. Sizing requirements to particles used to visualize the aircraft vortex wake. Trudy TsAGI 1996;2622:146–50 [in Russian].
[78] Ilina IP. Numerical simulation of the interaction between small particles and a vortex cluster during its evolution in the far vortex wake. Trudy TsAGI 1999;2641:389–95.
[79] Ilina IP, Soudakov VG. Investigation of the influence of a turbulent atmosphere on motion of small particles in the vortex wake behind an aircraft. Trudy TsAGI 1999;2641:396–400.
[80] Mikhailov Yu S. Experimental simulation of vortex wake influence on AON model in T-103 wind tunnel in TsAGI. Trudy TsAGI 1996;2622:188–96 [in Russian].
[81] Mikhailov Yu S. Vortex wake simulation in a wind tunnel. Trudy TsAGI 1999;2641:197–203.
[82] Matveev AV, Nazarov VV, Osminin RI. Experimental study into three-dimensional displacements of a flexible aircraft model under the action of gusts in wind-tunnel flow. Trudy TsAGI 1999;2641:274–82.
[83] Kuznetsov OA, Orlova TI. On calculating aircraft dynamic load by vortex wake. Trudy TsAGI 1996;2622:169–77 [in Russian].
[84] Kuznetsov OA, Orlova TI. Evaluation of safe separation distances between aircraft from the strength standpoint. Trudy TsAGI 1997;2627:138–47.
[85] Kuznetsov OA, Orlova TI. Dynamics loading of the aircraft model induced by vortex gusts: experiment and computation. Trudy TsAGI 1997;2627:148–56.
[86] Kuznetsov OA, Orlova TI. Prediction of aircraft displacements in turbulent flow. Trudy TsAGI 1999;2641:265–73.
[87] Kuzmin VP. Analysis of the vortex wake effect on an aircraft in landing approach. Trudy TsAGI 1999;2641:227–38.
[88] Bobylev AV, Glushkov NN, Gryazin VE. Mathematical model of interaction with the vortex wake for a set of geometrically similar aircraft. Trudy TsAGI 1999;2641:239–46.